Electronic Supplementary Material (ESI) for Sustainable Energy & Fuels.

Supplementary Material

Dual-strategy of interface and reconstruction engineering to boost efficient alkaline water and seawater oxidation

Dongxue Guo, Mengya Zong, Zhe Zhao, Cunzheng Fan, Danhong Wang*

TKL of Metal and Molecule Based Material Chemistry, College of Chemistry, School of Materials Science and Engineering, Nankai University, Tianjin 300350, China

*Corresponding author.

E-mail address: dhwang@nankai.edu.cn (D.-H. Wang)

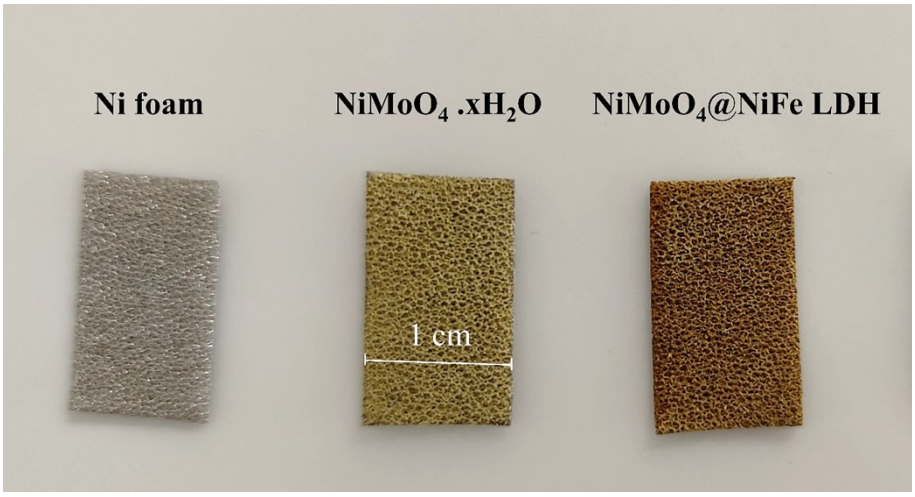

Fig. S1. Optical photographs of Ni foam, $NiMoO_4.xH_2O$ and $NiMoO_4$@NiFe LDH.

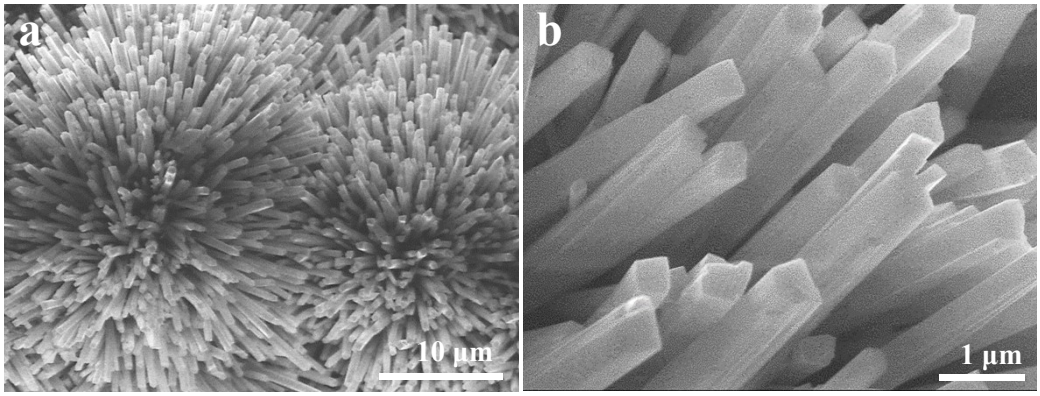

Fig. S2. SEM images at low (a) and high (b) magnifications for $NiMoO_4.xH_2O$.

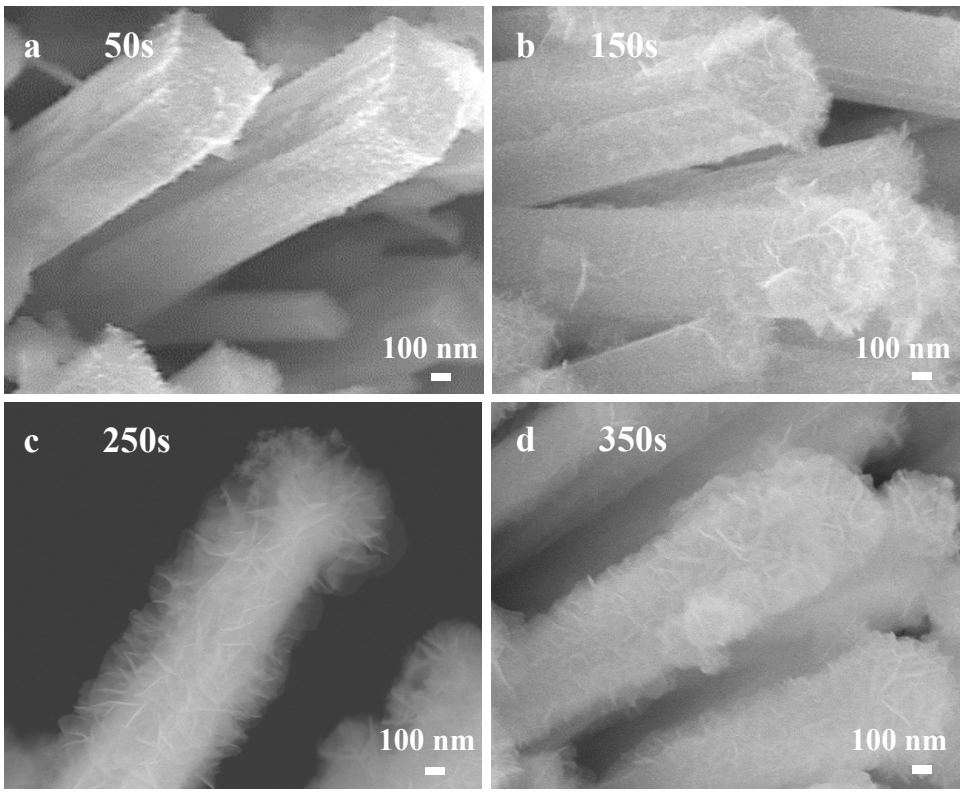

Fig. S3. SEM images of $NiMoO_4$@NiFe LDH with different electrodeposition time of NiFe LDH.

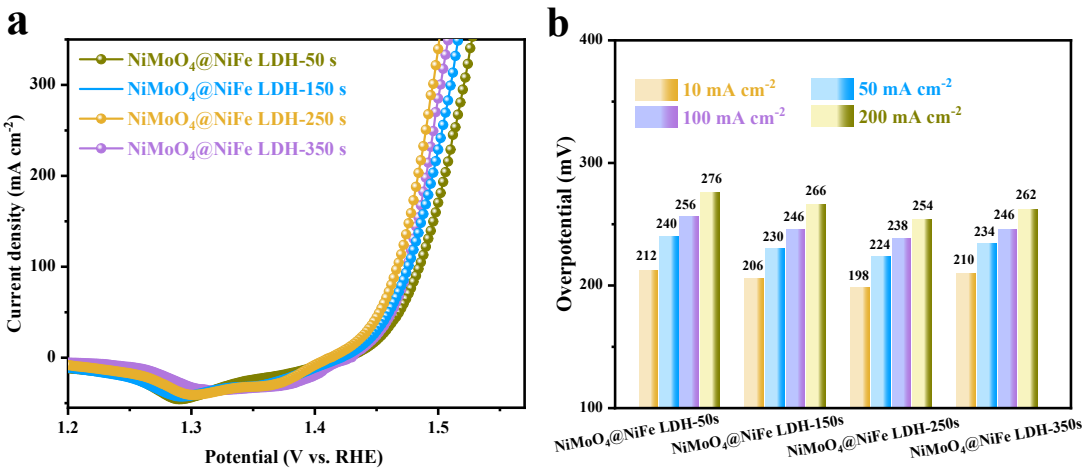

Fig. S4. OER polarization curves of $NiMoO_4$@NiFe LDH with different electrodeposition time of NiFe LDH tested in 1 M KOH electrolyte. (b) Comparison of the overpotentials required for these catalysts to attain current densities of 10, 50, 100, and 200 mA cm^{-2} for OER.

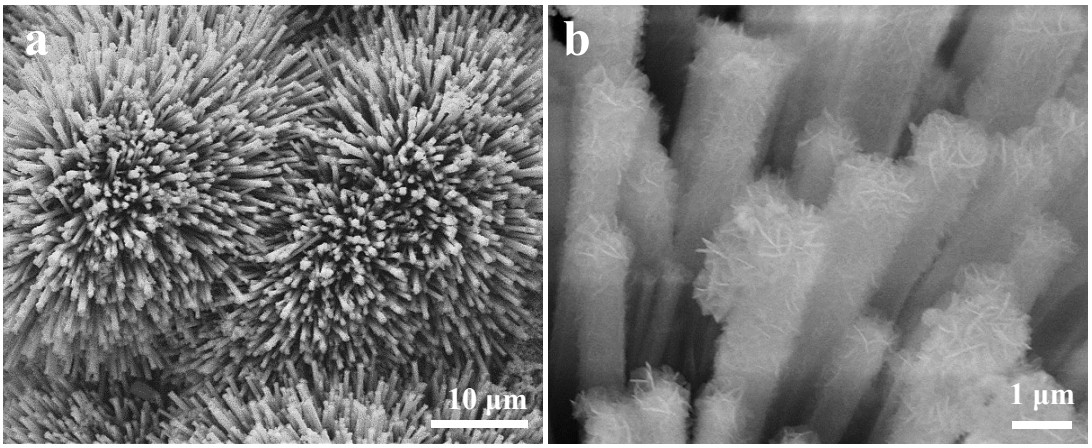

Fig. S5. SEM images at low (a) and high (b) magnifications for $NiMoO_4$@NiFe LDH-250 s.

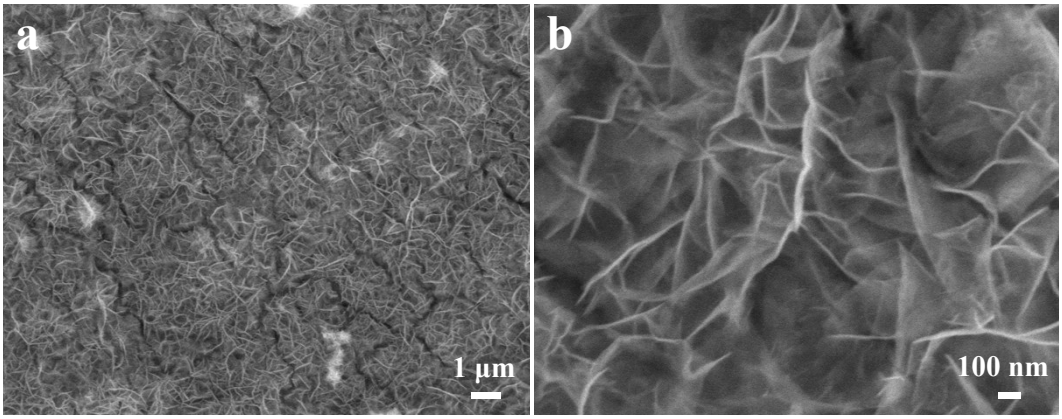

Fig. S6. SEM images at low (a) and high (b) magnifications for NiFe LDH/NF.

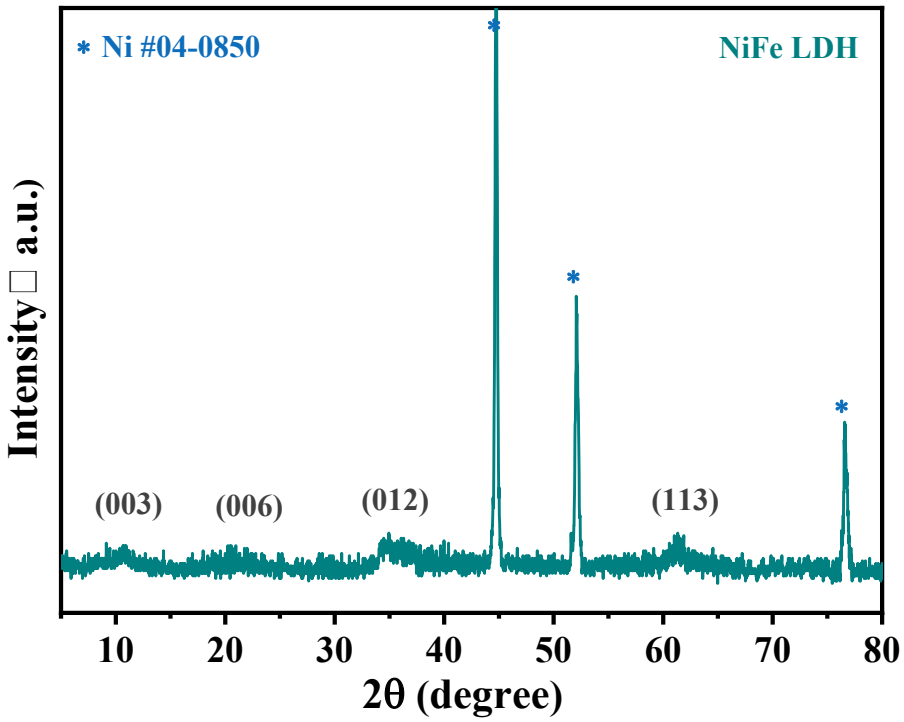

Fig. S7. XRD patterns of NiFe LDH.

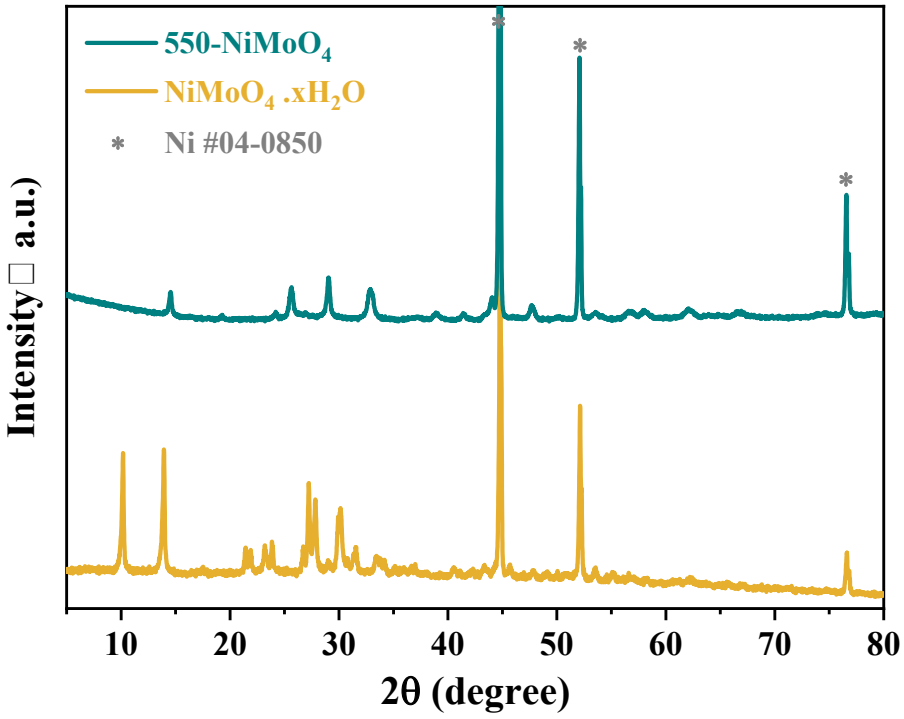

Fig. S8. XRD patterns of annealed $NiMoO_4$ and $NiMoO_4.xH_2O$.

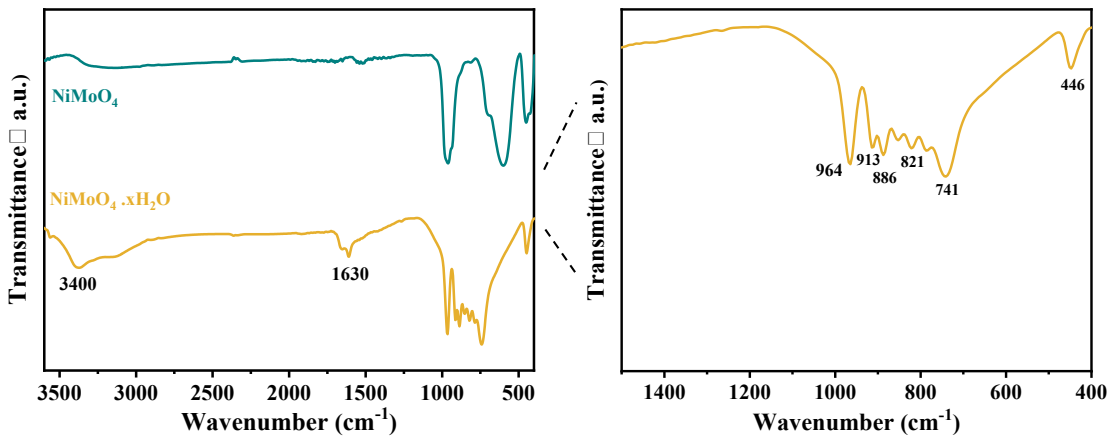

Fig. S9. FTIR spectra of annealed $NiMoO_4$ and $NiMoO_4.xH_2O$ with the magnified spectra.

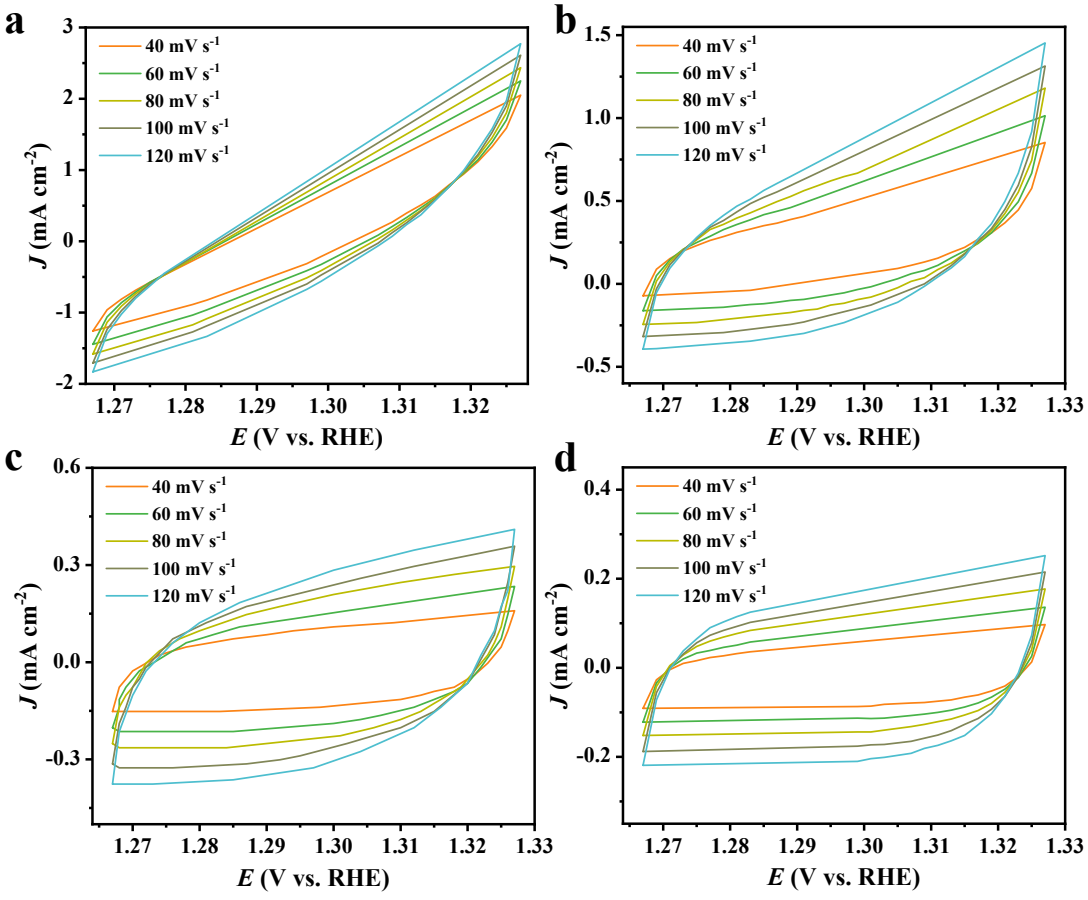

Fig. S10. Typical cyclic voltammograms at different scan rates. (a) $NiMoO_4$@NiFe LDH, (b) $NiMoO_4.xH_2O$, (c) NiFe LDH and (d) NF with scan rates ranging from 40 mV/s to 120 mV/s with an interval point of 20 mV/s.

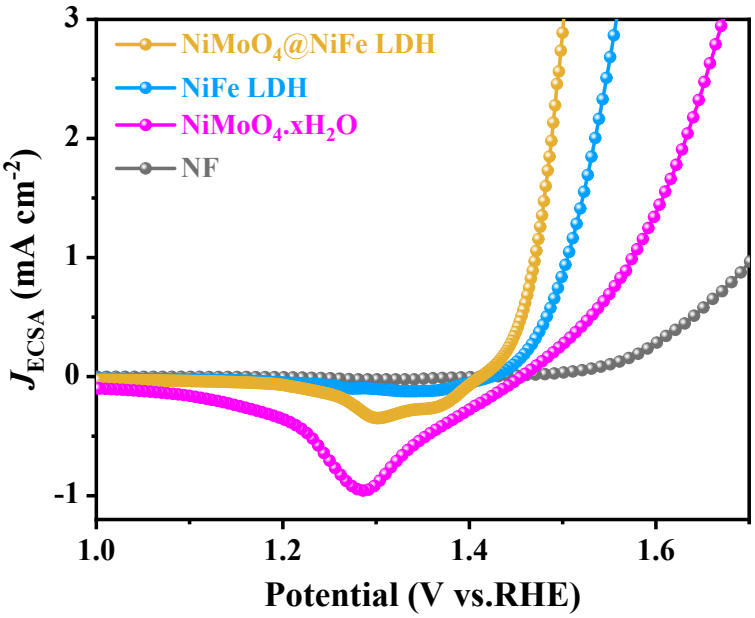

Fig. S11. ECSA normalized polarization curves for $NiMoO_4$@NiFe LDH, NiFe LDH, $NiMoO_4.xH_2O$ and NF.

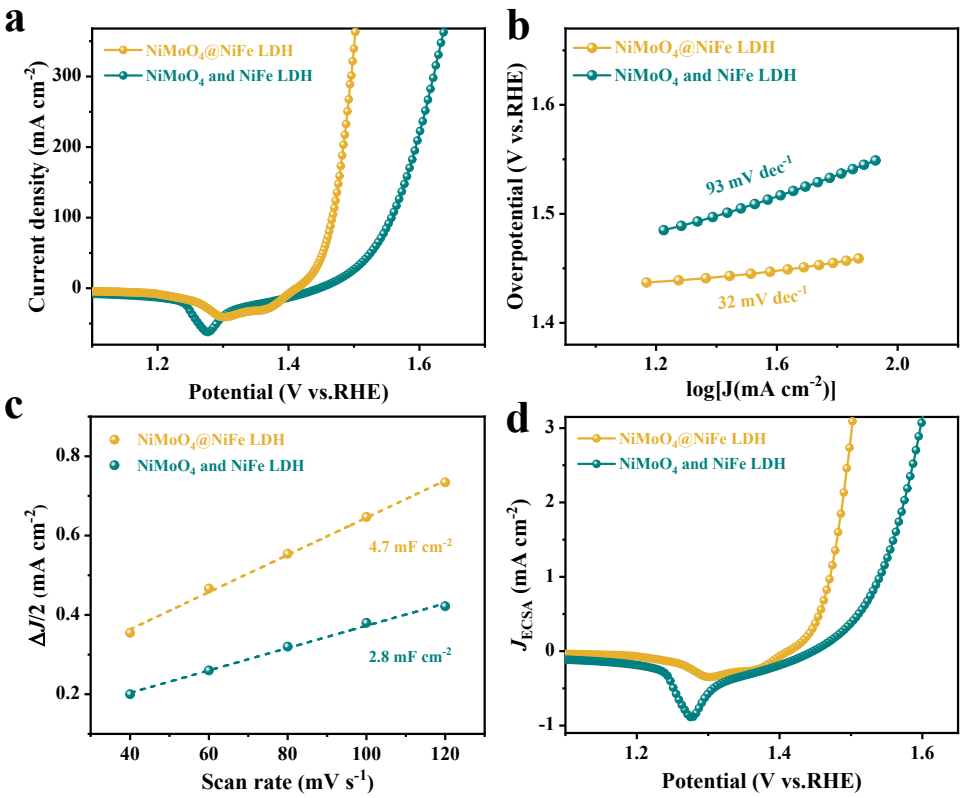

Fig. S12. (a) OER Polarization curves, (b) corresponding Tafel plots, (c) electrical double layer capacitance (C_{dl}) and (d) ECSA normalized polarization curves of core-shell NiMoO4@NiFe LDH catalysts and physically mixed composite.

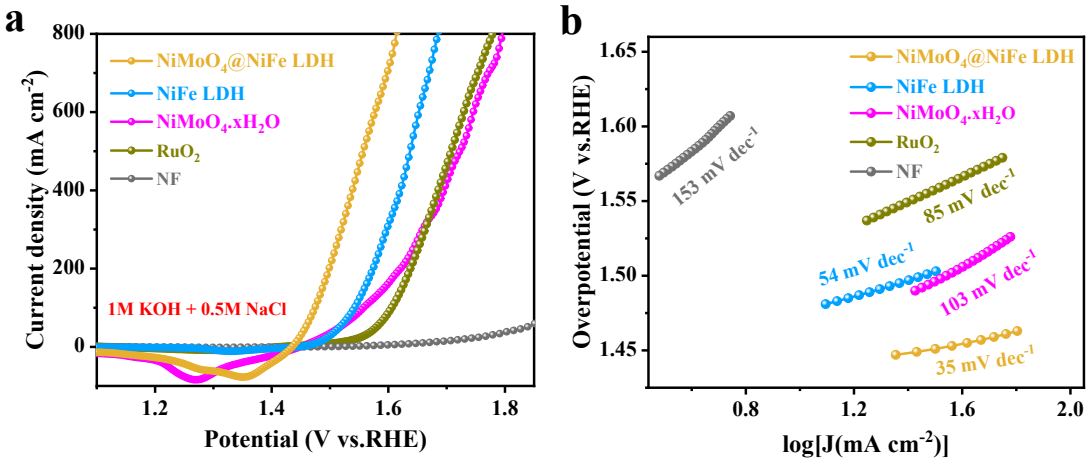

Fig. S13. (a) OER Polarization curves and (b) corresponding Tafel plots of the studied catalysts in 1M KOH + 0.5 M NaCl electrolyte.

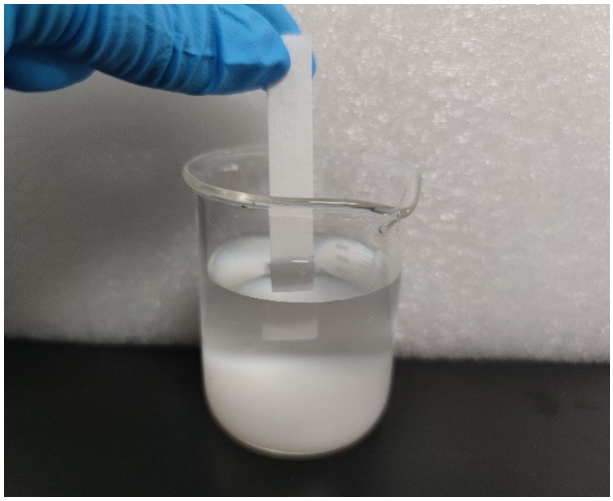

Fig. S14. The digital photograph of the results for ClO^- formation in 1 M KOH seawater electrolyte after OER stability testing of $NiMoO_4$@NiFe LDH at 100 mA cm^{-2} for 80 h. The formation of hypochlorite (ClO^-) was examined via the potassium iodide starch paper.

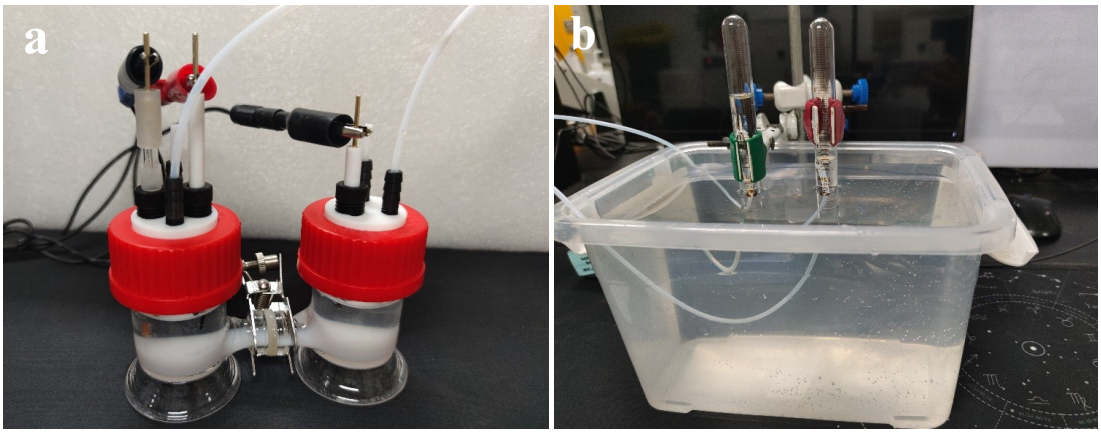

Fig. S15. Photograph of the (a) H type cell and (b) gas collection device.

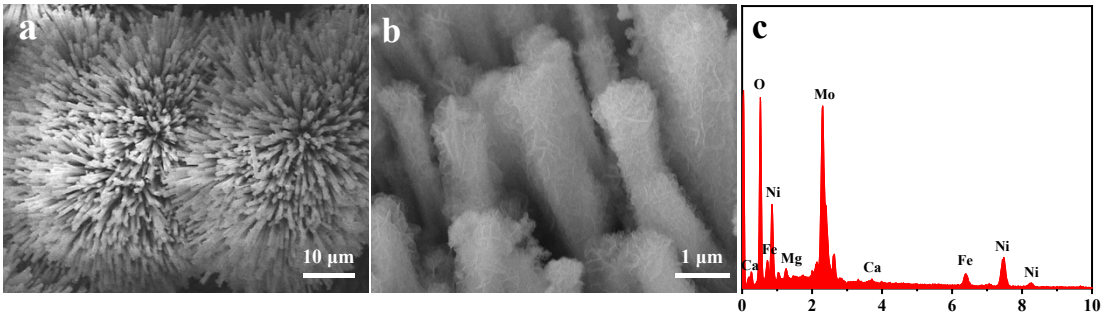

Fig. S16. (a-b) SEM images and (c) EDS spectrum of $NiMoO_4$@NiFe LDH catalyst after immersion in natural seawater for 15 days.

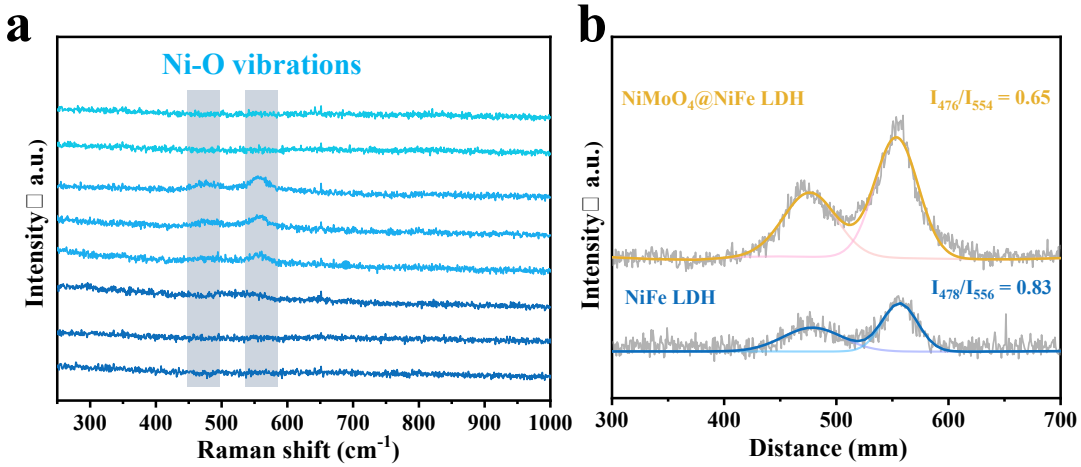

Fig. S17. (a) In-situ Raman spectra of NiFe LDH in 1 M KOH during the OER process. (b) Raman bands of NiMoO4@NiFe LDH and NiFe LDH measured at 1.6 V versus RHE.

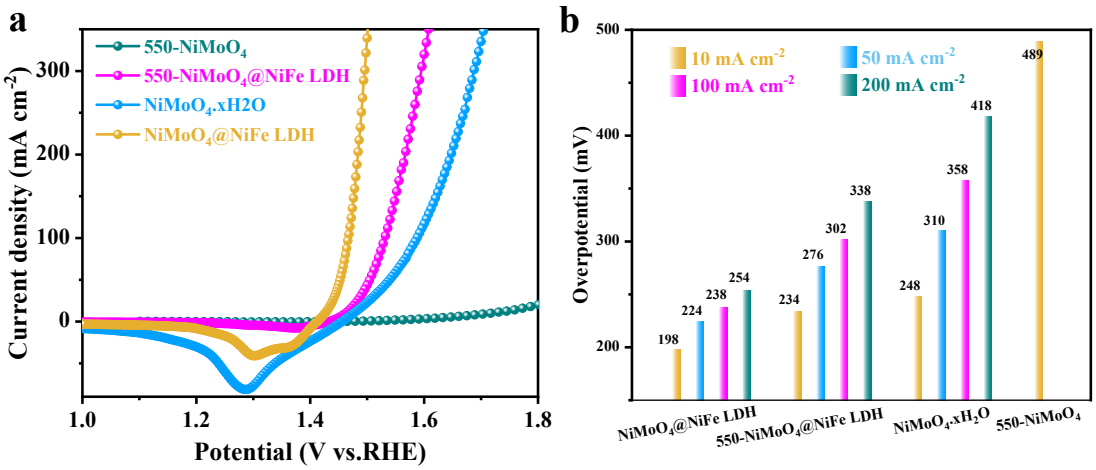

Fig. S18. OER polarization curves of $NiMoO_4.xH_2O$, $NiMoO_4$@NiFe LDH, annealed $NiMoO_4$ and annealed $NiMoO_4$@NiFe LDH in 1 M KOH electrolyte. (b) Comparison of the overpotentials required for these catalysts to attain current densities of 10, 50, 100, and 200 mA cm^{-2} for OER.

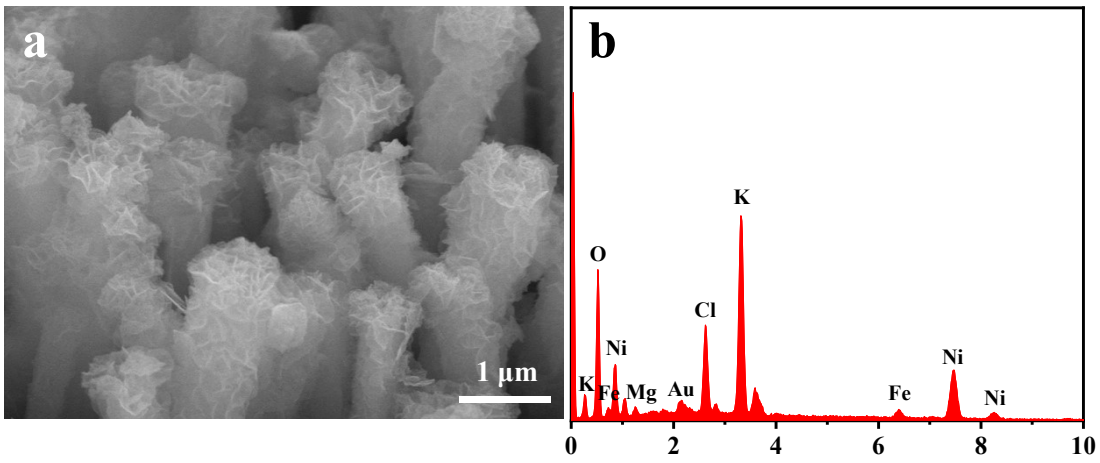

Fig. S19. (a) SEM images and (b) EDS spectrum of $NiMoO_4$@NiFe LDH catalyst after OER test in 1 M KOH seawater.

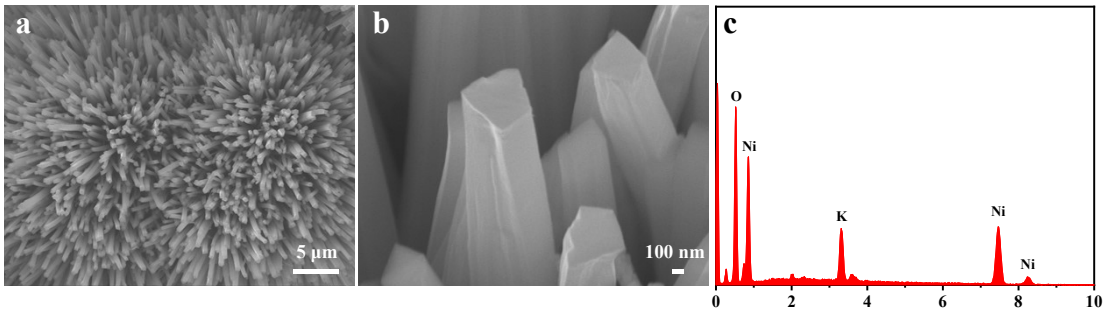

Fig. S20. (a-b) SEM images and (c) EDS spectrum of $NiMoO_4.xH_2O$ catalyst after OER test in 1 M KOH.

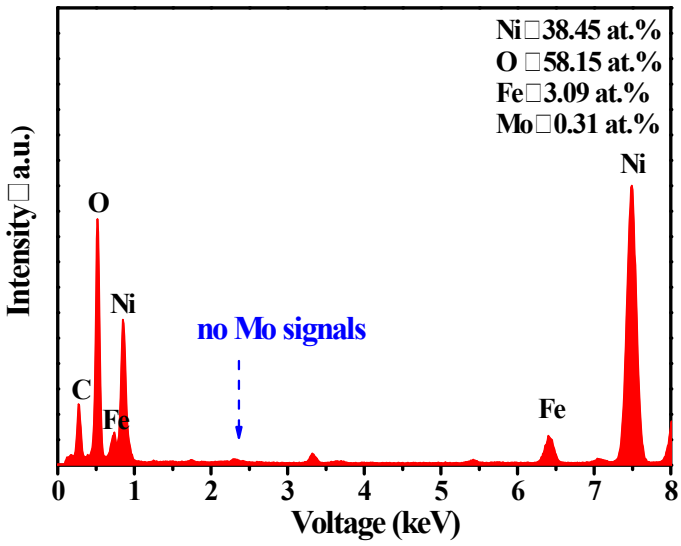

Fig. S21. EDS map sum spectrum of $NiMoO_4$@NiFe LDH catalyst after OER test in 1 M KOH.

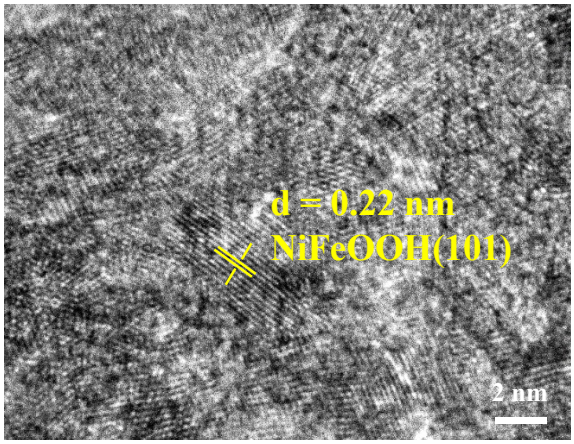

Fig. S22. The high-magnification TEM image of $NiMoO_4$@NiFe LDH catalyst after OER test in 1 M KOH.

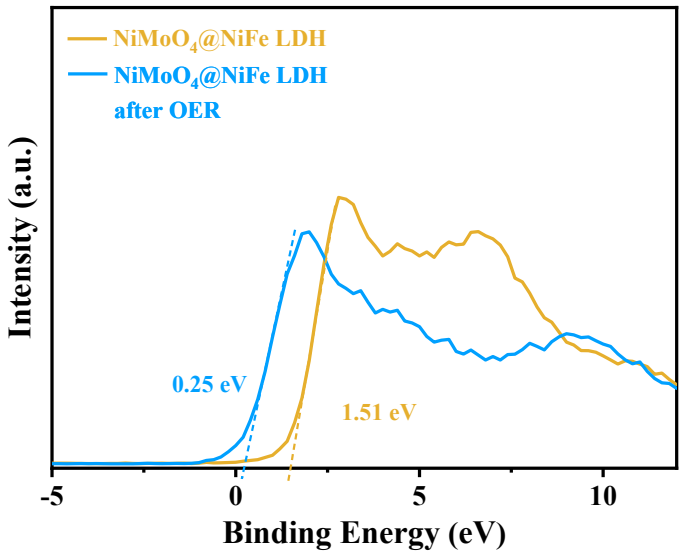

Fig. S23. Valence band spectra of $NiMoO_4$@NiFe LDH before and after OER catalysis in 1 M KOH.

Table S1. Comparison of OER performance of $NiMoO_4$@NiFe LDH with some previously reported NiFe-based catalysts in 1.0 M KOH solution.

Catalysts	Electrolyte	η (mV) at 10 mA cm^{-2}	Tafel slope (mV/dec)	Reference
$NiMoO_4$@NiFe LDH	**1.0 M KOH**	**198**	**32**	***This work***
Fe-doped β-$Ni(OH)_2$	1.0 M KOH	219	53	[1]
hcp-NiFe@NC	1.0 M KOH	226	41	[2]
$Fe_{0.052}$Ni-POMo	1.0 M KOH	255.3 ± 1.6	43.8	[3]
NiFe-based SURMOFs	0.1 M KOH	300	44.3	[4]
NiFe-LDH	1.0 M KOH	275	56.7	[5]
Ni Fe MOF	0.1 M KOH	240	34	[6]
NiOOH/FeOOH NBs	1.0 M KOH	246	41	[7]
$Ni_{0.8}Co_{0.1}Fe_{0.1}$OxHy	1.0 M KOH	239	45.4	[8]
$Ni^{II}Fe^{III}$@NC	1.0 M KOH	360	81	[9]
NiFe@N doped carbon	0.1 M KOH	350	56	[10]
Fe/(Ni)OOH	1.0 M KOH	290	32	[11]
$Ni_{2/3}Fe_{1/3}$ LDH	1.0 M KOH	310	76	[12]
Fe-S-$NiMoO_4/MoO_3$	1.0 M KOH	212	41	[13]
Ni (Fe)OxHy	1.0 M KOH	218 ± 5	31 ± 4	[14]
NiCoFe-P-NP@NiCoFe-PBA	1.0 M KOH	223	78	[15]

NiFe/NiFe−OH	1.0 M KOH	222	41	[16]
MnCo-CH@NiFe-OH	1.0 M KOH	186	49	[17]
a-NiFe-OH/NiFeP/NF	1.0 M KOH	199	39	[18]

Table S2. Comparison of OER performance of $NiMoO_4$@NiFe LDH with some previously reported catalysts for seawater oxidation.

Catalysts	**Electrolyte**	**η (mV) at 100 mA cm^{-2}**	**η (mV) at 500 mA cm^{-2}**	**Reference**
$NiMoO_4$@NiFe LDH	**1 M KOH seawater**	**251**	**349**	***This work***
Ni_3S_2/Co_3S_4	1 M KOH seawater	360	440	[19]
Ni_3FeN@C	1 M KOH seawater	283	351	[20]
MoS_2-$(FeNi)_9S_8$	1 M KOH seawater	256	329	[21]
Gd-Mn_3O_4@ CuO-$Cu(OH)_2$	1 M KOH seawater	-	400	[22]
$Ir_1/Ni_{1.6}Mn_{1.4}O_4$	0.5 M KOH seawater	330	-	[23]
B-Co_2Fe LDH	1 M KOH seawater	310	376	[24]
NiFe LDH	1 M KOH seawater	247	296	[25]
CoPx@FeOOH	1 M KOH seawater	283	337	[26]

S-(Ni,Fe)OOH	1 M KOH seawater	300	398	[27]
Ni_3S_2/Fe-NiPx	1 M KOH seawater	290	336	[28]

References

1. T. Kou, S. Wang, J. L. Hauser, M. Chen, S. R. J. Oliver, Y. Ye, J. Guo and Y. Li, ACS Energy Letters, 2019, 4, 622-628.

2. C. Wang, H. Yang, Y. Zhang and Q. Wang, Angew. Chem. Int. Ed., 2019, 58, 6099-6103.

3. X. Liu, F. Xia, R. Guo, M. Huang, J. Meng, J. Wu and L. Mai, Adv. Funct. Mater., 2021, 31, 2101792.

4. S. Hou, W. Li, S. Watzele, R. M. Kluge, S. Xue, S. Yin, X. Jiang, M. Döblinger, A. Welle, B. Garlyyev, M. Koch, P. Müller-Buschbaum, C. Wöll, A. S. Bandarenka and R. A. Fischer, Adv. Mater., 2021, 33, 2103218.

5. M. Liu, L. Kong, X. Wang, J. He and X.-H. Bu, Small, 2019, 15, 1903410.

6. J. Duan, S. Chen and C. Zhao, Nature Communications, 2017, 8, 15341.

7. P. Yan, Q. Liu, H. Zhang, L. Qiu, H. B. Wu and X.-Y. Yu, Journal of Materials Chemistry A, 2021, 9, 15586-15594.

8. Q. Zhao, J. Yang, M. Liu, R. Wang, G. Zhang, H. Wang, H. Tang, C. Liu, Z. Mei, H. Chen and F. Pan, ACS Catalysis, 2018, 8, 5621-5629.

9. L. Du, L. Luo, Z. Feng, M. Engelhard, X. Xie, B. Han, J. Sun, J. Zhang, G. Yin, C. Wang, Y. Wang and Y. Shao, Nano Energy, 2017, 39, 245-252.

10. Z. Zhang, Y. Qin, M. Dou, J. Ji and F. Wang, Nano Energy, 2016, 30, 426-433.

11. H. Zhong, J. Wang, F. Meng and X. Zhang, Angew. Chem. Int. Ed., 2016, 55, 9937-9941.

12. W. Ma, R. Ma, C. Wang, J. Liang, X. Liu, K. Zhou and T. Sasaki, ACS Nano, 2015, 9, 1977-1984.

13. Y. Zhang, H. Guo, J. Ren, X. Li, W. Ren and R. Song, Applied Catalysis B: Environmental, 2021, 298, 120582.

14. Q. Xu, H. Jiang, X. Duan, Z. Jiang, Y. Hu, S. W. Boettcher, W. Zhang, S. Guo and C. Li, Nano Lett., 2021, 21, 492-499.

15. G. Zhang, Y. Li, X. Xiao, Y. Shan, Y. Bai, H.-G. Xue, H. Pang, Z. Tian and Q.

Xu, Nano Lett., 2021, 21, 3016-3025.

16. W. Zhu, W. Chen, H. Yu, Y. Zeng, F. Ming, H. Liang, Z. Wang, Appl. Catal. B: Environ., 2020, 278, 119326.

17. Y. Zeng, Z. Cao, J. Liao, H. Liang, B. Wei, X. X, H. Xu, J. Zheng, W. Zhu, L. Cavallo, Z. Wang, Appl. Catal. B: Environ., 2021, 292, 120160.

18. H. Liang, A. N. Gandi, C. Xia, M. N. Hedhili, D. H. Anjum, U. Schwingenschlögl, and H. N. Alshareef, ACS Energy Lett., 2017, 2, 1035-1042.

19. C. Wang, M. Zhu, Z. Cao, P. Zhu, Y. Cao, X. Xu, C. Xu and Z. Yin, Applied Catalysis B: Environmental, 2021, 291, 120071.

20. B. Wang, M. Lu, D. Chen, Q. Zhang, W. Wang, Y. Kang, Z. Fang, G. Pang and S. Feng, Journal of Materials Chemistry A, 2021, 9, 13562-13569.

21. S. Song, Y. Wang, S. Zhou, H. Gao, X. Tian, Y. Yuan, W. Li and J. Zang, ACS Applied Energy Materials, 2022, 5, 1810-1821.

22. T. ul Haq, S. Mansour and Y. Haik, ACS Applied Materials & Interfaces, 2022, 14, 20443-20454.

23. N. Wen, Y. Xia, H. Wang, D. Zhang, H. Wang, X. Wang, X. Jiao and D. Chen, Advanced Science, 2022, n/a, 2200529.

24. L. Wu, L. Yu, Q. Zhu, B. McElhenny, F. Zhang, C. Wu, X. Xing, J. Bao, S. Chen and Z. Ren, Nano Energy, 2021, 83, 105838.

25. M. Ning, L. Wu, F. Zhang, D. Wang, S. Song, T. Tong, J. Bao, S. Chen, L. Yu and Z. Ren, Materials Today Physics, 2021, 19, 100419.

26. L. Wu, L. Yu, B. McElhenny, X. Xing, D. Luo, F. Zhang, J. Bao, S. Chen and Z. Ren, Applied Catalysis B: Environmental, 2021, 294, 120256.

27. L. Yu, L. Wu, B. McElhenny, S. Song, D. Luo, F. Zhang, Y. Yu, S. Chen and Z. Ren, Energy & Environmental Science, 2020, 13, 3439-3446.

28. X. Luo, P. Ji, P. Wang, X. Tan, L. Chen and S. Mu, Advanced Science, 2022, 9, 2104846.